Early detonation by sprouted mossy fibers enables aberrant dentate network activity

William D. Hendricks[1,3], Gary L. Westbrook[2] & Eric Schnell[3,4]

[1]Neuroscience Graduate Program; [2]Vollum Institute; Oregon Health and Science University, Portland, OR, 97239; USA; [3]Department of Anesthesiology and Perioperative Medicine; Oregon Health and Science University, Portland, OR, 97239; USA; [4]VA Portland Health Care System; Portland, OR, 97239; USA

*Corresponding Author
Eric Schnell, MD, PhD
schneler@ohsu.edu
3710 SW US Veterans Hospital Rd, P3ANES
Portland, OR 97239

In temporal lobe epilepsy, sprouting of hippocampal mossy fiber axons onto dentate granule cells creates a recurrent excitatory network. Unlike mossy fibers projecting to CA3, these sprouted mossy fiber synapses display prominent short-term depression, which could limit their participation in epileptiform activity. However, we reveal that a lack of tonic adenosine-mediated inhibition at these synapses contributes to an elevated probability of glutamate release and enables reverberant circuit activity.

Mossy fibers contacting CA3 pyramidal cells have a low initial probability of release (P_r), and rapidly facilitate with repetitive activation[1]. These "detonator" synapses strongly drive post-synaptic cell firing[2]. In epilepsy, recurrent sprouting of mossy fiber synapses with these properties could be highly epileptogenic, particularly given the proximal dendritic location of sprouted mossy fiber terminals onto other granule cells[3]. However, sprouted mossy fibers rapidly depress during repetitive activation[4], which might seem to limit the extent with which they could drive seizure activity[5].

The functional contribution of mossy fiber sprouting to epileptogenesis remains controversial[5-8], thus we directly examined the contribution of sprouted mossy fiber activation to epileptiform activity in acute slices prepared from epileptic mice (see methods). To isolate

sprouted mossy fiber inputs from other inputs, we used DcxCre::ChR2 mice to specifically activate sprouted mossy fibers while recording from Channelrhodpsin2 (ChR2)-negative (unlabeled) granule cells[4, 9] (Fig. 1a-c; Supplementary Fig. 1). Optogenetic stimulation evoked EPSCs in dentate granule cells only from pilocarpine-treated mice (Fig. 1d,e; also see ref. 4). Postsynaptic cells filled were with dye during recordings and did not have hilar basal dendrites (0 of 32 cells; Fig. 1c), indicating that LED-evoked responses originated from recurrent (sprouted mossy fiber) synaptic inputs.

In addition to monosynaptic sprouted mossy fiber – GC (smf-GC) EPSCs, we frequently observed LED-evoked epileptiform activity after single light pulses (Fig. 1d, right). Cells with EPSC bursts had similar intrinsic properties as cells with single or no evoked recurrent EPSCs (R_i, input resistance: cells without bursts, 610 ± 47 MΩ; cells with bursts, 527 ± 77 MΩ; unpaired t-test, $t_{30} = 0.9711$, $p = 0.3392$; C_m, cell capacitance: non-bursts, 51.5 ± 3.8 pF; bursts, 46.8 ± 3.8; unpaired t-test, $t_{30} = 0.8302$, $p = 0.4130$). Subsequent EPSC peaks during bursts had high jitter (Supplementary Fig. 2), indicative of polysynaptic network activation. Furthermore, as optogenetic stimulation only triggered single spikes in ChR2-expressing granule cells (number of AP: 0.98 ± 0.09, n = 5 cells), this suggests sprouted mossy fiber activation also drove multiple rounds of polysynaptic activity, through recurrent excitatory connectivity in the dentate gyrus. Given the paucity of surviving hilar mossy cells observed in the pilocarpine model as well as in several other models of epilepsy[10-12], this recurrent excitation likely originated through activation of sprouted mossy fibers.

Unlike healthy mossy fiber – CA3 synapses[1], sprouted mossy fiber synapses exhibit profound frequency-dependent short-term depression during repetitive activation (Supplementary Fig. 3, see also ref. 4), which may limit their ability to drive multiple rounds of postsynaptic firing[5]. Thus, we compared patterns of spike generation in response to a short 10

Hz train of optogenetic stimulation in CA3 pyramidal cells or unlabeled granule cells. In striking contrast to synaptic facilitation and delayed spike generation at mf-CA3 synapses, 10 Hz stimulation induced spikes only at the beginning of the train at sprouted mossy fiber synapses (Fig. 1f,g). Importantly, the lack of change in action potential fidelity indicated that this firing pattern did not result from a failure to activate sprouted mossy fibers in epileptic brains (Supplemental Fig. 1) but rather resulted instead from reduced glutamate release later in the train. Despite the profound short-term synaptic depression at these synapses, activation of postsynaptic firing with single pulses was clearly sufficient to trigger multiple rounds of recurrent activation (Fig. 1d).

The frequency-dependent short-term depression and the robust initial recruitment of postsynaptic cell firing during recurrent activation (Fig. 1g) could result from a high initial probability of release (P_r) at sprouted mossy fiber synapses. To directly test whether sprouted mossy fibers have an increased P_r, we measured use-dependent MK-801 block kinetics during activation of both types of mossy fiber synapses. Optogenetically-evoked NMDAR-mediated synaptic currents were isolated by voltage-clamping target cells to -70 mV in Mg^{2+} free ACSF in the presence of NBQX (10 μM) and SR95531 (10 μM) to block AMPA- and $GABA_A$-receptors, respectively. After baseline EPSC recording, LED stimulation was paused for 10 minutes while MK-801 (40 μM) was washed onto the slice and allowed to equilibrate. Upon resuming LED stimulation (0.05 Hz), MK-801 progressively inhibited NMDAR-EPSCs from smf-GC and mf-CA3 synapses (Fig. 2a). The rate of decay was faster for sprouted mossy fiber synapses (Fig. 2b), indicating a higher P_r at sprouted mossy fiber synapses (Fig. 2c). Interestingly, MK-801 block rate at smf-GC synapses was better fit by a double-exponential decay model (Fig. 2b) whereas at mf-CA3 synapses, a single exponential model was sufficient, suggesting increased synaptic heterogeneity at sprouted mossy fiber synapses[13]. Overall, the increased P_r at

sprouted mossy fiber synapses likely exacerbates granule cell firing and therefore the spread of recurrent excitation in epileptic brains.

Extracellular adenosine tonically inhibits neurotransmitter release at healthy mossy fiber synapses in CA3 via A1-type adenosine receptors (A_1Rs) located on mossy fiber boutons, and tonic activation of pre-synaptic A_1Rs contributes to the profound short-term facilitation at these synapses[14, 15]. As altered adenosine metabolism may be a contributing factor in epileptogenesis[16-18], we posited that sprouted mossy fibers might manifest an increased P_r due to a reduction in A_1R-mediated inhibition. To measure tonic A_1R-mediated inhibition of sprouted mossy fibers in epileptic mice, we washed on the selective high-affinity A_1R antagonist, 8-Cyclopentyl-1,3-dipropylxanthine (DPCPX, 200 nM) while recording sprouted mossy fiber-mediated responses. As expected for a pre-synaptic effect on A_1Rs, the DPCPX-induced increase in EPSC amplitudes at mf-CA3 synapses (Fig. 3a,b) coincided with decreased PPR (paired-pulse ratio, P_2/P_1: pre-DPCPX, 2.36 ± 0.37; post-DPCPX, 1.37 ± 0.12, n = 6; paired t-test, p = 0.0191). However, in contrast to the enhancement of synaptic transmission at healthy mf-CA3 synapses[14], DPCPX did not affect sprouted mossy fiber EPSCs (Fig. 3a,b), indicating a lack of tonic A_1R signaling.

To distinguish whether the lack of tonic A_1R-mediated inhibition at sprouted mossy fiber synapses resulted from an absence of adenosine receptors, we washed on the selective A_1R agonist, 2-Chloro-N^6-cyclopentyladenosine (CCPA, 1 μM). CCPA reduced sprouted mossy fiber EPSCs (Fig. 3c,d) and increased paired-pulse facilitation (Supplementary Fig. 4), indicating that A_1Rs were present and functional on sprouted mossy fiber terminals. Although CCPA decreased the probability of release at sprouted mossy fiber synapses, it did not restore frequency facilitation (Supplementary Fig. 5), suggesting that the molecular mechanisms underlying synaptic facilitation at mossy fiber terminals cannot be restored solely by increasing A_1R activation.

Finally, to test if reduced A_1R activation and increased P_r at sprouted mossy fiber synapses contributes to recurrent circuit activation, we determined the effect of A_1R activation in hippocampal slices from epileptic mice. When applied to slices demonstrating polysynaptic bursts after sprouted mossy fiber activation, the A_1R agonist CCPA reduced the number of EPSCs in the polysynaptic burst as well as the relative amount of charge transfer carried by the burst (Fig. 3e,f). Together, these data indicated that reduced A_1R activation at granule cell outputs contributes to hyperexcitability in the dentate gyrus in epileptic brains.

Notably, adenosine agonists can reduce the severity of seizures[19, 20]. Although seizure activity in epileptic brains likely results from multiple hyperexcitable circuit elements, the lack of tonic adenosine signaling in the dentate gyrus profoundly enhances sprouted mossy fiber transmission by setting a high P_r for glutamate release, shifting sprouted mossy fiber synapses from "conditional detonators" to "early detonators", which can drive recurrent circuit activation and bursts of EPSCs. Whether these recurrent circuits drive seizure activity *in vivo* has been debated[5, 6], however the extensive formation and properties of recurrent excitatory circuits provide avenues for buildup of excitation during seizures.

Acknowledgments

We wish to thank Drs. Zhi-Qi Xiong and Xuewen Cheng (Shanghai Institute for Neuroscience) for providing the DcxCreER^{T2} mouse line, and members of the Schnell and Westbrook laboratories for critical feedback and discussion on the manuscript. Research funding was provided by Department of Veterans Affairs, Veterans Health Administration, Office of Research and Development, Biomedical Laboratory and Development CDA-2 award 005-10S (ES); Department of Veterans Affairs Merit Review Award I01-BX002949 (ES); a Department of Defense CDMRP Award W81XWH-18-1-0598 (ES); a National Institutes of Health (NIH) Grant F31-NS098597 (WDH); NIH Grant R01-NS080979 (GLW); the Ellison

Medical Foundation (GLW); and NIH Grant P30-NS061800 (Oregon Health and Science University Advanced Light Microscopy Core). The contents of this manuscript do not represent the views of the U.S. Department of Veterans Affairs or the United States government.

Author Contributions

WDH, GLW, and ES designed the research; WDH performed the experiments and analyzed data; WDH, GLW, and ES provided sources of funding; WDH and ES wrote the manuscript.

Competing interests

The authors declare no competing interests.

References

1. Nicoll, R.A. & Schmitz, D. *Nature Reviews Neuroscience* **6**, 863-876 (2005).
2. Vyleta, N.P., Borges-Merjane, C. & Jonas, P. *eLife* **5** (2018).
3. Okazaki, M.M., Evenson, D.A. & Nadler, J.V. *Journal of Comparative Neurology* **352**, 515-534 (2018).
4. Hendricks, W.D., Chen, Y., Bensen, A.L., Westbrook, G.L. & Schnell, E. *The Journal of Neuroscience* **37**, 5722-5735 (2017).
5. Smith, B.N. *Epilepsy Currents* **17**, 379-380 (2017).
6. Buckmaster, P.S. *Issues in Clinical Epileptology: A View from the Bench* 161-168 (Springer, Dordrecht, 2014).
7. Longo, B.M. & Mello, L.E.A.M. *Neuroscience Letters* **226**, 163-166 (1997).
8. Longo, B.M. & Mello, L.E.A.M. *Epilepsy Research* **32**, 172-182 (1998).
9. Cheng, X.*, et al. Cell Research* **21**, 338-349 (2011).
10. Borges, K. *Experimental Neurology* **182**, 21-34 (2003).
11. Buckmaster, P.S. & Dudek, F.E., 20.
12. Mello, L.E.A.M.*, et al. Epilepsia* **34**, 985-995 (2005).
13. Rosenmund, C., Clements, J. & Westbrook, G. *Science* **262**, 754-757 (1993).
14. Moore, K.A., Nicoll, R.A. & Schmitz, D. *Proceedings of the National Academy of Sciences* **100**, 14397-14402 (2003).
15. Fedele, D.E.*, et al. Brain* **128**, 2383-2395 (2005).
16. Boison, D. *Progress in Neurobiology* **84**, 249-262 (2008).
17. Sandau, U.S.*, et al. Journal of Neuroscience* **36**, 12117-12128 (2016).
18. Williams-Karnesky, R.L.*, et al. J Clin Invest* **123**, 3552-3563 (2013).
19. Amorim, B.O.*, et al. Epilepsy & Behavior* **61**, 168-173 (2016).
20. Gouder, N., Fritschy, J.-M. & Boison, D. *Epilepsia* **44**, 877-885 (2018).
21. Shibley, H. & Smith, B.N. *Epilepsy Research* **49**, 109-120 (2002).

Figures and Figure Legends:

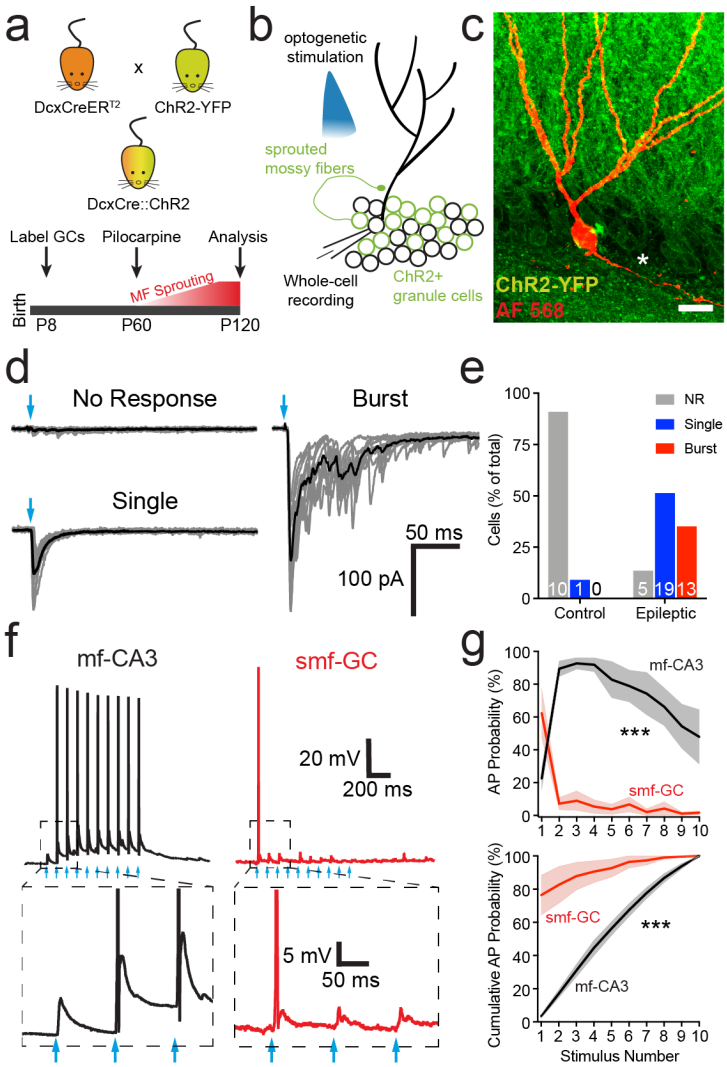

Figure 1: Stimulation of sprouted mossy fibers triggers spiking in post-synaptic dentate granule cells. **a,** Experimental design for granule cell labeling and induction of epileptic mossy fiber sprouting. DcxCreER^{T2} mice were bred with conditional ChR2-YFP (Ai32) reporter mice (top) and given tamoxifen (TAM) at P8 to turn on reporter gene expression (bottom). At 2 months (P60), mice were given pilocarpine to induce seizures and mossy fiber sprouting or kept as controls. All analysis was at P120. **b,** Whole-cell recordings were performed on ChR2-negative dentate granule cells and sprouted mossy fiber axons were stimulated with blue (470 nm) LED light delivered through the objective. **c,** Representative confocal image of a recorded granule

cell filled with AlexaFluor 568 (50 μM) during whole-cell recording (levels and gamma adjusted for clarity). Star designates mossy fiber axon; no basal dendrites were present (scale, 10 μm). **d,** Example traces from cells with no response (top left), single EPSCs (bottom left), and epileptiform bursts (right) after single optogenetic stimulation of ChR2+ granule cells (blue arrows). Scale bar on right applies to all traces. **e,** The frequency of cells with single EPSCs (Single), and EPSC bursts (Burst) in epileptic mice was greater than controls (Chi-square, $p < 0.0001$). Number of cells in each category are listed on the graph. **f,** Representative current clamp recordings during mossy fiber – CA3 (mf-CA3, black trace) and sprouted mossy fiber – granule cell (smf-GC, red trace) activation by 10 Hz, 10 pulse LED trains (blue arrows). Dashed boxes represent insets (below) highlighting facilitation of mf-CA3 EPSPs (left) and depression of smf-GC EPSPs (right). **g,** Action potential (AP) probability (top) is shifted to the first stimulus after smf-GC activation relative to mf-CA3 activation (mf-CA3, n = 6 cells; smf-GC, n = 8 cells, 2-way RM ANOVA, $F_{1,12} = 85.68$, $p < 0.0001$; Sidak's multiple comparisons test, Stimulus 1, $p = 0.0048$, Stimuli 2 – 9, all $p < 0.0001$, Stimulus 10, $p = 0.0006$). Summary data presented as mean ± SEM. ***$p < 0.001$

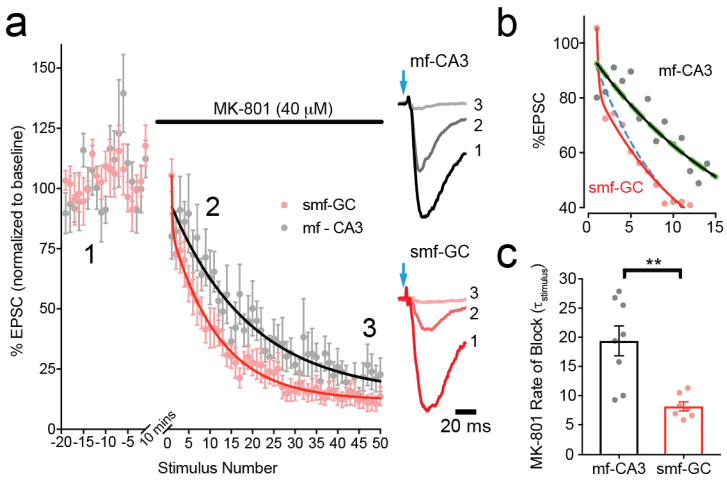

Figure 2: Elevated P_r at sprouted mossy fiber synapses. **a,** Probability of release was measured from the kinetics of use-dependent MK-801 block of NMDAR-mediated EPSCs during 0.05 Hz LED stimulation. Averaged and normalized responses (left) are plotted before and after bath application of MK-801 (40 μM; mf-CA3, n = 8; smf-GC, n = 7). Representative, peak-scaled NMDAR EPSC averages (right) were taken during baseline, shortly after resuming LED stimulation, and at the end of the experiment, numbered 1, 2, 3, respectively. **b,** Same as in (a), but only showing the first 15 sweeps. Single (solid lines) and double (dashed lines) exponential fits are plotted for smf-GC (red and blue) and mf-CA3 (black and green). Sprouted mossy fibers are better fit by double exponential decays (extra sum of squares F-test, $F_{2,395} = 5.07$, $p = 0.0067$) whereas mf-CA3 synapses are fit identically by single and double models. **c,** Average rate of MK-801 block measured in individual cells. MK-801 rate of block was significantly faster at sprouted mossy fiber synapses (unpaired t-test, $t_{13} = 3.942$, $p = 0.0017$), indicating higher P_r. All data are presented as mean ± s.e.m. **$p < 0.01$

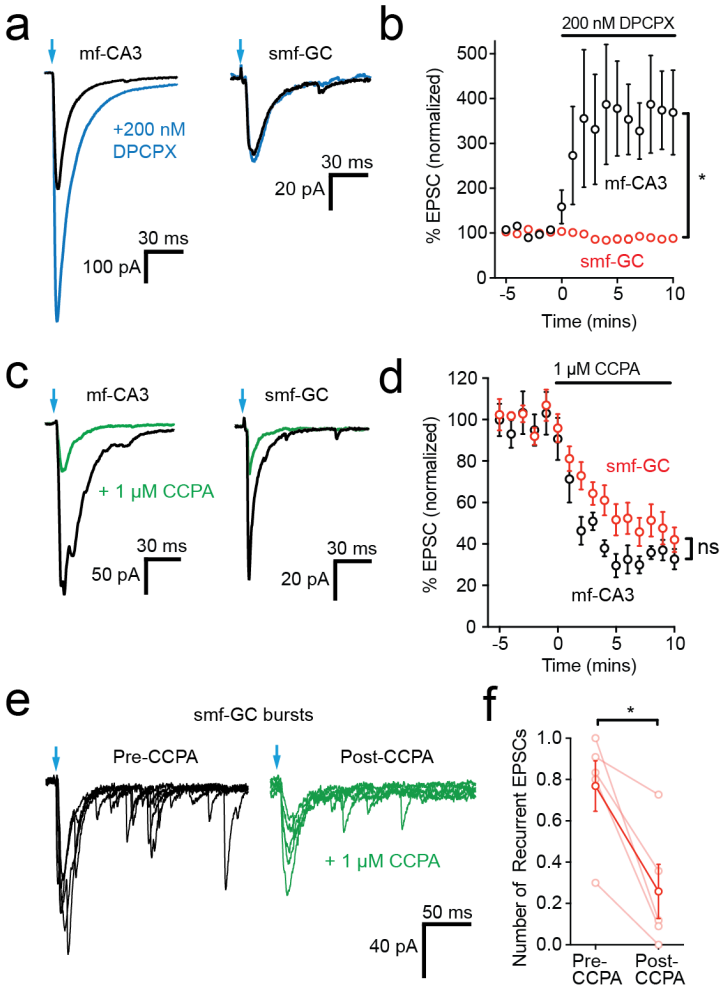

Figure 3: Lack of tonic adenosine contributes to increased release probability. **a,** Mossy fiber – CA3 (left) and sprouted mossy fiber-GC (right) EPSCs before (black traces) and after (blue traces) washing on the adenosine 1a receptor (A_1R) antagonist, DPCPX (200 nM). Bath application of DPCPX facilitates mf-CA3 EPSCs (n = 8 cells, paired t-test, t_7 = 5.77, p = 0.0007), but has no effect on EPSC amplitudes at smf-GC synapses (n = 5 cells, paired t-test, t_4 = 1.39, p = 0.2364). **b,** Normalized EPSC amplitudes of mf-CA3 (black, n = 8 cells) and smf-GC (red, n = 5 cells) responses before and during DPCPX administration (unpaired t-test, t_{11} = 3.63 p = 0.0040). **c,** The A_1R agonist CCPA (1 μM) inhibits both mf-CA3 (left) and smf-GC (right) EPSCs similarly (baseline, black example traces; CCPA, green traces). **d,** Normalized mf-CA3 (black) and smf-GC (red) EPSC amplitudes during CCPA application, demonstrating intact A_1R

responses at both synapses (mf-CA3, n = 7 cells, smf-GC, n = 12 cells; unpaired t-test, t_{17} = 1.08, p = 0.2954). **e,** Adenosine A_1R agonism inhibits recurrent polysynaptic network activity evoked by single pulse optogenetic stimulation of sprouted mossy fibers. Examples are 5 consecutive EPSC traces overlaid from the same cell, pre- and post-CCPA (black and green, respectively). **f,** Quantification of EPSC burst inhibition by CCPA at smf-GC synapses. CCPA (1 μM) reduces the mean number of recurrent EPSCs during a burst (number of recurrent EPSCs per epoch, n = 5 cells, t_4 = 3.963, p = 0.0166). Summary data presented as mean ± SEM. *p < 0.05

Methods

Animals

All experiments were carried out in accordance with local, state, and federal guidelines, and protocols were approved by the OHSU Institutional Animal Care and Use Committee. Housing was provided by Oregon Health & Science University's Department of Comparative Medicine vivarium accredited by the Association for Assessment and Accreditation of Laboratory Animals. To generate DcxCre::ChR2 mice, homozygous *doublecortin-CreER*^{T2} (line F18; RRID:MGI:5438982) mice were bred with homozygous *Gt(ROSA)26Sor*$^{tm32(CAG-COP4*H134R/EYFP)Hze}$ (Ai32; RRID:IMSR_JAX:012569) and used as previously described[4,9]. Briefly, Cre-mediated combination was induced by tamoxifen (TAM) at P8 (2 injections, 12 hours apart, 20 mg/kg in corn oil, i.p.), to permanently label granule cells with ChR2-eYFP in DcxCre::ChR2 heterozygous mice. Seizures were induced in two-month-old male mice with 325 mg/kg i.p. pilocarpine (Cayman Chemicals) after pre-treating with an i.p. injection of scopolamine methyl bromide (Sigma-Aldrich). Seizures were graded on the modified Racine Scale[21]; status epilepticus (SE) was defined when a mouse had 3 or more Racine Grade 3 seizures, followed by continuous grade 2 seizing. Following 2 hours of SE, seizures were terminated with diazepam (10 mg/kg i.p.) (Hospira, Inc.) and given soft food and i.p. injections of 5% glucose in 0.45% normal saline to aid in recovery. Mice that did not develop SE were humanely killed and excluded from further analysis.

Slice Physiology

Acute brain slices for *ex vivo* electrophysiology were prepared similarly as previously described. In brief, four-month-old male DcxCre::ChR2 mice were anesthetized with 4% isoflurane, followed by injection of 1.2% avertin (Sigma-Aldrich). Mice were transcardially perfused with 10 mL of ice-cold N-methyl-D-glucamine (NMDG)-based cutting solution, containing the following (in mM): 93 NMDG, 30 NaHCO3, 24 glucose, 20 HEPES, 5 Na-

ascorbate, 5 N-acetyl cysteine, 3 Na-pyruvate, 2.5 KCl, 2 thiourea, 1.2 NaH2PO4, 10 MgSO4, and 0.5 CaCl2. Mice were rapidly decapitated, hippocampus dissected, and 300 μm transverse hippocampal sections were prepared in ice-cold NMDG solution with a Leica VT1200S vibratome. Hippocampal dissections were omitted for CA3 recordings and 300 μm sagittal slices were prepared to preserve pyramidal cells. Slices from both preparations recovered in warm NMDG cut solution for 15 mins followed by standard ACSF at room temperature for 1 hour prior to recording.

Dentate granule cell and CA3 pyramidal cell recordings were obtained with 3-5 MΩ borosilicate glass pipettes filled with a Cs^+-based internal solution for voltage-clamp experiments, or a K^+-based internal solution for current-clamp experiments. The Cs^+-based internal solution contained the following (in mM): 113 Cs-gluconate, 17.5 CsCl, 10 HEPES, 10 EGTA, 8 NaCl, 2 Mg-ATP, 0.3 Na-GTP, 0.05 Alexa Fluor 568, pH adjusted to 7.3 with CsOH, with a final osmolarity of 295 mOsm; QX-314-Cl (5 mM; Tocris Bioscience) was included to block unclamped action potentials. The K^+-based internal solution contained (in mM): 130 K-gluconate, 20 KCl, 10 HEPES, 4 Mg-ATP, 0.3 Na-GTP, 0.1 EGTA, 0.05 AlexaFluor 568, pH adjusted to 7.2 KOH, with a final osmolarity of 295 mOsm. Granule cells and CA3 pyramidal cells were identified with infrared differential interference contrast imagining on an Olympus BX-51WI microscope. Whole-cell recordings were obtained by making high-resistance seals (>5 GΩ) and applying brief suction. Cells were filled with Alexa Fluor 568 dye to visually confirm cell type and assess for presence of hilar basal dendrites on dentate granule cells in epileptic mice. Series resistance was uncompensated and cells with a >30% change in series resistance were excluded from analysis. Liquid junction potential was 8 mV and was uncorrected. For current-clamp recordings, minimal negative current was injected if necessary to maintain a resting potential of -70 mV in dentate granule cells and CA3 pyramidal cells.

Pulses of blue LED-powered (Thorlabs) light (1 ms, 470 nm, 8 mW/cm^2, 0.05 Hz) were delivered through a 40x water immersion objective, targeted at the stratum lucidum for CA3 recordings and inner molecular layer for granule cell recordings. Stimulation frequency was modified for various experiments as noted in the text. Signals were amplified with an AxoPatch 200B amplifier (Molecular Devices), low-pass Bessel-filtered at 5 kHz, and digitized and sampled at 10 kHz using a NIDAQ (National Instruments) analog-to-digital board. Data were captured using a custom Igor Pro 5.05 (Wavemetrics) script and NIDAQmx (National Instruments) plugins. For presentation of EPSCs, a 2 kHz Gaussian filter was applied, *post-hoc.*

Statistical Analysis

Curve fitting and EPSC trace averaging was carried out in Igor Pro 8 (Wavemetrics) using built-in and custom functions, respectively. Epileptiform burst activity (multiple EPSCs to single stimulus) was determined by eye, aided by fitting a single exponential curve to the initial decay and identifying delayed EPSC peaks rising above the decay fit line. Charge transfer was calculated using the trapezoidal area function in Igor Pro. Peak detection was implemented in Igor Pro by identifying zero-point crossings of thresholded peaks on the first-order derivative of the EPSC. Additional statistical analysis was performed in Prism 8 (GraphPad). Normality was tested with the Shapiro-Wilk normality test prior to statistical test selection. No statistical tests were used to pre-determine sample-size. Experimenters were not blinded to experimental condition. Paired and unpaired t-tests were used for normally distributed datasets; Mann-Whitney and Wilcoxon matched-pairs signed rank test were used for non-parametric datasets. For all experiments, significance was determined by $p < 0.05$ (*$p < 0.05$, **$p < 0.01$, ***$p < 0.001$). All summary data is presented as mean ± SEM.

Code Availability

Custom IgorPro scripts are available upon reasonable request from the corresponding author.

Data Availability

All primary data supporting the findings in this manuscript are available upon reasonable request from the corresponding author.

Supplementary Figures:

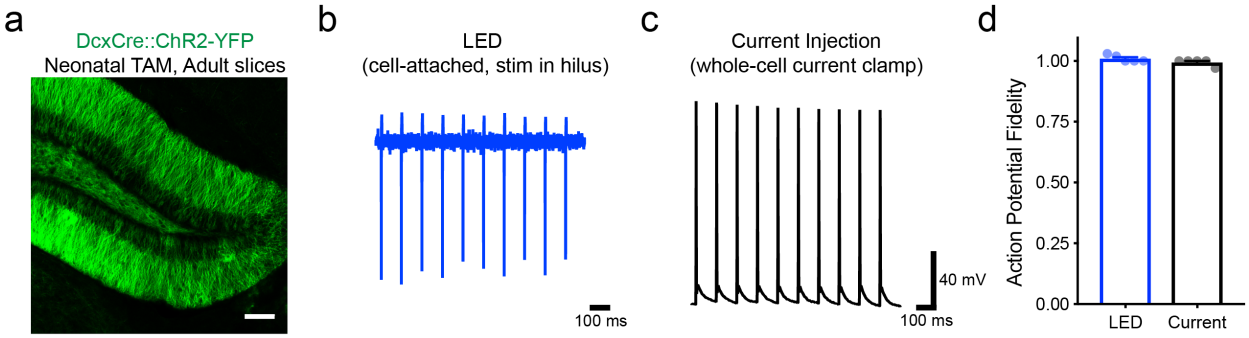

Supplementary Figure 1: Action potential fidelity at 10 Hz stimulation in epileptic mice.

a) Single confocal image from DcxCre::ChR2 mouse given tamoxifen neonatally (P6) and perfused at 4 months, demonstrating mature granule cell labeling. Scale bar is 100 μm.

b) Example trace from a cell-attached recording of a ChR2 expressing dentate granule cell from an epileptic mouse reliably firing action potentials in response to optogenetic stimulation at 10 Hz (1 ms LED pulse, 470 nm, 8 mW/cm^3). LED light was delivered via a 40x objective placed over the hilus to trigger antidromic action potential propagation and avoid direct stimulation of ChR2-expressing cell bodies.

c) Example trace from a whole-cell current clamp recording of a dentate granule cell from an epileptic mouse, demonstrating that these cells reliably fire actions potentials during repeated brief current injections (1 ms, 500 pA, 10 Hz).

d) Summary of action potential fidelity upon optogenetic (blue; n = 5) or current-injection (black; n = 5) stimulus trains. Actual potential fidelity potted as number action potentials evoked per LED stimulus. Data plotted as mean ± SEM.

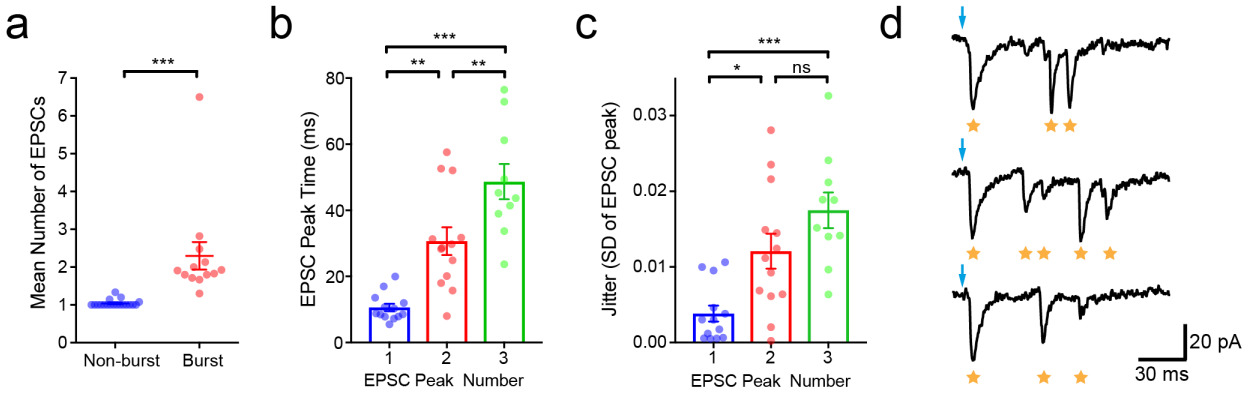

Supplementary Figure 2: EPSC onset and jitter analysis during EPSC bursts

a) Cells with bursts have greater average number of EPSC peaks (Mean number of peaks: Non-burst, n = 19; Burst, n = 13; unpaired t-test, $t_{30} = 4.18$, $p = 0.0002$).

b) EPSC peak times of the first 3 peaks during an EPSC burst (EPSC peak onset times: Peak 1, n = 13 cells; Peak 2, n = 13 cells; Peak 3, n = 10 cells; One-way ANOVA, $F_{2,33} = 25.1$, $p < 0.0001$; Tukey's test, Peak 1 vs. Peak 2, $p = 0.0010$, Peak 1 vs. Peak 3, $p < 0.0001$, Peak 2 vs. Peak 3, $p = 0.0060$). Note increased variability of onset time in subsequent peaks, further characterized in (b).

c) Jitter (trial to trial variability of EPSC onsets, as standard deviation) taken from the first 3 peaks in an EPSC burst is increased after the first EPSC peak (EPSC jitter: Peak 1, n = 13; Peak 2, n = 13; Peak 3, n = 10; One-way ANOVA, $F_{2,33} = 12.0$, $p = 0.0001$; Tukey's test, Peak 1 vs. Peak 2, $p = 0.0105$; Peak 1 vs. Peak 3, $p < 0.0001$; Peak 2 vs. Peak 3, $p = 0.1544$). High variability in second and third EPSC peaks within a burst suggest that they result from polysynaptic activity.

d) Three consecutive traces taken from a cell with EPSC bursts. Optogenetic stimulation (blue arrow) evoked an initial EPSC (likely monosynaptic) followed by variably timed burst EPSCs (likely polysynaptic). Gold stars designate detected EPSCs.

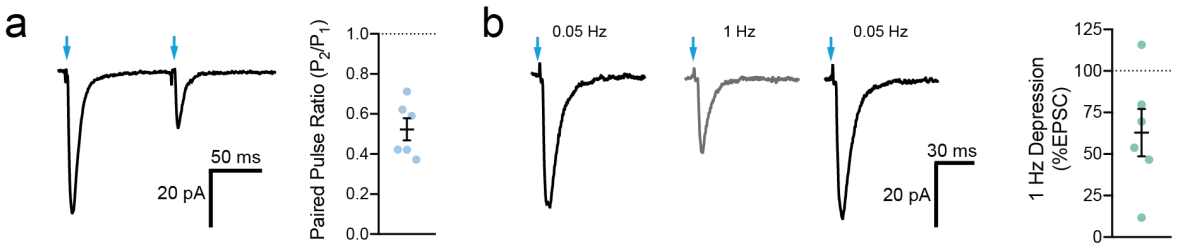

Supplementary Figure 3: Sprouted mossy fibers exhibit paired-pulse depression and 1 Hz stimulation.

(a) Example trace of paired pulse stimulation (100 ms ISI) of sprouted mossy fibers axons (left) and summary plot (right). Sprouted mossy fibers have a low paired-pulse ratio (PPR: 0.523 ± 0.06, n = 6). Blue arrows mark optogenetic stimulation.

(b) Example average EPSC responses during baseline (0.05 Hz, left trace), 1 Hz stimulation (middle trace), and recovery (0.05 Hz, right trace). Summary data is plotted on the right. Sprouted mossy fibers display prominent depression during 1 Hz stimulation (%EPSC of baseline: 62.9 ± 14.3%, n = 6). Blue arrows mark optogenetic stimulation.

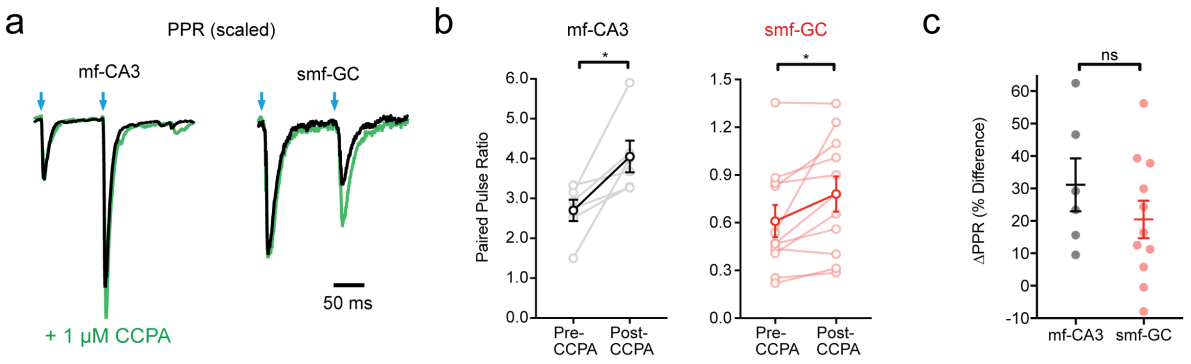

Supplementary Figure 4: The A_1R agonist CCPA increases the paired pulse ratio at both mossy fiber – CA3 and sprouted mossy fiber – GC synapses.

(a) Representative EPSCs from paired-pulse experiments (100 ms ISI) from both mf-CA3 (left) and smf-GC (right) recordings before (black traces) and after (green traces) bath application of CCPA (1 μM, A_1R agonist). Traces are scaled and normalized to the first EPSC peak. Larger relative EPSC peaks on the second pulse in CCPA indicates an increased paired-pulse ratio (PPR).

(b) Quantification of paired-pulse experiments exemplified in (a). CCPA increases the PPR in both mf-CA3 (left) and smf-GC (right) experiments (PPR, mf-CA3: n = 6, paired t-test, t_5 = 3.195, p = 0.0241; PPR, smf-GC: n = 11, paired t-test, t_{10} = 2.74, p = 0.0208). Group averages are overlaid over individual experiments.

(c) Change in PPR from bath application of CCPA (% Difference) is similar for mf-CA3 and smf-GC synapses (ΔPPR: mf-CA3, n = 6; smf-GC, n = 11, unpaired t-test, t_{15} = 1.082, p = 0.2962).

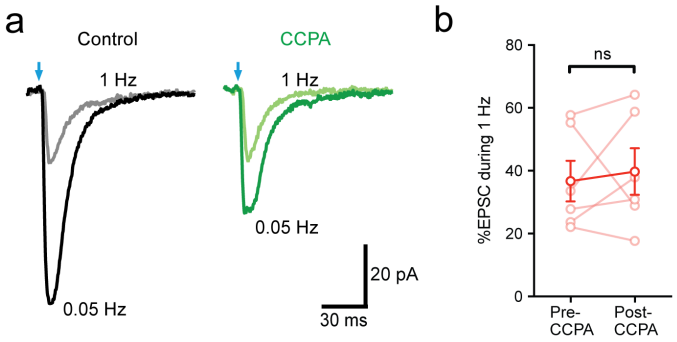

Supplementary Figure 5: Restoring A_1R tone with CCPA does not restore frequency-dependent facilitation at sprouted mossy fiber synapses.

(a) Example traces taken at baseline stimulation frequency (0.05 Hz, darker traces) and during 1 Hz frequency trains (lighter traces) before (black traces) and after (green traces) bath application of CCPA (1 μM), demonstrating decreased EPSC amplitudes when evoked at 1 Hz. Examples are taken from the same cell/experiment. Scale bar is the same for both examples.

(b) Quantification of experiments shown in (a). Bath application of CCPA does not alter EPSC depression during 1 Hz LED trains (% EPSC during 1 Hz, 50 pulse trains: pre-CCPA, n = 6; t_5 = 0.422, paired t-test, p = 0.6905).